International Journal for Multiscale Computational Engineering, 4(5&6)791–801(2006)

A Space-Time Multiscale Method for Molecular Dynamics Simulations of Biomolecules

Aiqin Li, Haim Waisman, and Jacob Fish*

Scientific Computational Research Center, Rensselaer Polytechnic Institute,
Troy, NY 12180, USA

ABSTRACT

A novel multiscale approach for molecular-dynamics simulations is developed. The goal of this method is to reduce the time cost of molecular-dynamics simulations without loss of accuracy in the quantities of interest. The proposed approach consists of the waveform relaxation scheme aimed at capturing the high-frequency motions and a coarse-scale solution in space and time aimed at resolving smooth features (in both space and time domains) of the system. The use of proper orthogonal decomposition (POD) modes at the coarse-grained level has been found to accelerate convergence of the waveform relaxation scheme. The accuracy and efficiency of this method are reported by applying it to a model problem of chain of α-D-glucopyranose monomers.

KEYWORDS

waveform relaxation, space-time multiscale, multigrid, proper orthogonal decomposition (POD), biomolecules

*Address all correspondence to fishj@rpi.edu, Phone 1-518-276-6191

1. INTRODUCTION

Molecular motions involve a large number of atoms and take place over a great range of time scales. For example, local motions such as atomistic fluctuations and sidechain motion are on the order of femtoseconds (10^{-15} s) while a large-scale motion such as protein folding occurs at the time level of 10^{-7} to 10^{4} s [1,2]. Because of the presence of high-frequency motions, the typical time step in a molecular-dynamics (MD) simulation is on the order of femtoseconds (10^{-15} s). These characteristics make a numerical molecular-dynamics simulation a computationally intensive task.

Since the large number of force evaluations is the most time-consuming part in almost all molecular-dynamics simulations, most of the research on the acceleration of molecular-dynamics simulations has been focused on the efficient evaluation of forces. To efficiently calculate the forces associated with non-bonded interactions, Van der Waals interaction and electrostatic forces, several schemes have been developed. For electrostatic interactions, the developed algorithms include the Ewald summation [3], the particle-particle/particle-mesh (PPPM) method [4], and the fast multipole algorithms (FMAs) [5]. Also a cutoff radius is used to exclude from the force calculations those atom pairs that are at the distance greater than the cutoff distance [6]. The common techniques used for short range interactions include the Verlet list, the cell (or linked) list, and their combination. The interested reader is referred to [7] for an overview of these methods. Molecular simulations can also be accelerated by increasing the integration time step. Since the time step is limited by the rapidly varying motions, an obvious approach is to eliminate the high-frequency motions. In [8], Andersen developed an algorithm called rattle to fix the distances between certain atom pairs so that the high-frequency bond-stretching motions are left out. Another commonly used approach is to employ a variable time-step methods such as the multiple time step (MTS) [9]. Using the force-splitting MTS method reduces the number of evaluations of slowly varying force components. However, so far, the increase in the integration time steps have been quite modest [10].

An alternative approach based on the space-time variational multilevel principle was recently developed in [11]. The method consists of the waveform relaxation scheme aimed at capturing the high-frequency response of atomistic vibrations and a coarse-scale solution to resolve smooth features of the discrete medium. The waveform relaxation method has been used to efficiently integrate large systems of ODEs on parallel computers [11,12]. Multigrid methods have been applied to molecular simulations in [13–15].

One of the main challenges in devising an efficient multilevel approach is to construct the coarse-scale problem. A well-known approach is the coarse-grained molecular dynamics (CGMD) method [16]. In [11], the formulation of the coarse-grained model was directly derived from the fine scale using Hamilton's principle on the subspace of normal modes. These normal modes were calculated from the Hessian matrix of the system potential energy.

In this paper, a novel multilevel method is developed. Based on the idea of space-time multilevel method described in [11], proper orthogonal decomposition (POD) modes are employed to construct the prolongation operator instead of normal modes. Briefly stated, POD modes are optimal with respect to energy content associated with each mode. For the detailed physical interpretation of POD modes see [17–19]. The reduced-order model (ROM) based on POD modes has been successfully applied to a chain of glucopyranose monomers in [20], where it was shown that the nonlinear ROM based on POD modes provides a good approximation for the original system, while the nonlinear reduced-order model based on normal modes is less accurate in modeling the molecules with a strong nonlinearity. With the reduced-order system, the computational cost can be significantly reduced. In this paper, we consider a chain of glucopyranose monomers in order to study the performance of the proposed POD-based space-time multiscale method.

2. MODAL DESCRIPTION

Generally, the molecular-dynamics system can be constructed by means of dynamic equilibrium consideration or Hamilton's principle as

$$\begin{cases} M\ddot{d} = F^{\text{int}}(d) + F^{\text{ext}} \\ d(0) = d_0 \\ \dot{d}(0) = v_0 \end{cases} \tag{1}$$

where d is a vector of atom positions, M is the mass matrix, F^{ext} is a vector of external forces, and $F^{\text{int}} = -\nabla U(d)$ is the internal force vector defined as the negative gradient of the potential energy, $U(d)$.

2.1 The Waveform Relaxation Scheme

Currently, parallel computers are becoming a major computational resource for large-scale system simulations. Because of this, more attention has been paid to the use of the waveform-relaxation (WR) method in molecular-dynamics simulations. The WR method decouples the original system into smaller subsystems and then solves the subsystems independently. Two versions of the WR method are widely used for highly nonlinear systems.

The first one is a direct extension of the linear WR formulations, the so-called waveform-relaxation Newton (WRN) method [21] written in the MD context as

$$\begin{cases} m_i \ddot{d}_i^{v+1} = F^{\text{int}}(d_1^v, \ldots, d_{i-1}^v, d_i^{v+1}, d_{i-1}^v, \ldots, d_N^v) \\ \qquad\qquad + F^{\text{ext}} \\ d_i^{v+1}(0) = d_0 \\ \dot{d}_i^{v+1}(0) = v_0 \end{cases} \tag{2}$$

for every atom i in the system. The superscripts, v and $v+1$, are the iteration counters within a time window $t \in [t_0, t_n]$.

An alternative approach similar to Gauss-Seidel splitting is based on updating internal forces using the information already calculated from the iteration $v+1$. Mathematically, the system is written as

$$\begin{cases} m_i \ddot{d}_i^{v+1} = F^{\text{int}}(d_1^{v+1}, \ldots, d_{i-1}^{v+1}, d_i^{v+1}, d_{i-1}^v, \ldots, d_N^v) \\ \qquad\qquad + F^{\text{ext}} \\ d_i^{v+1}(0) = d_0 \\ \dot{d}_i^{v+1}(0) = v_0 \end{cases} \tag{3}$$

The Gauss-Seidel type of approach leads to faster convergence rates, obviously at the expense of more limited parallelization. The second variant is known as the waveform Newton (WN) [21,22]. The idea is to approximate the internal forces in Eq. (1) as

$$F^{\text{int}} = F^{\text{int}}(d^v) - D(d^v)(d^{v+1} - d^v) \tag{4}$$

where $D(d^v(t))$ is the Hessian matrix obtained from the second derivative of the potential function

$$D_{ij} = \frac{\partial^2 U(d(t))}{\partial d_i \partial d_j} \tag{5}$$

Substituting Eq. (4) into Eq. (1) gives

$$\begin{cases} M\ddot{d}^{v+1} + D(d^v)d^{v+1} = F^{\text{int}}(d^v) \\ \qquad\qquad + D(d^v)d^v + F^{\text{ext}} \\ d^{v+1}(0) = d_0 \\ \dot{d}^{v+1}(0) = v_0 \end{cases} \tag{6}$$

This system of equations can be integrated over the time interval $t \in [t_0, t_n]$ using the Newmark predictor-corrector algorithm [23].

The WR iteration is terminated when the maximum residual in a time window is smaller than a specified tolerance,

$$\max\{\| r^{v+1}(t) \|_2\} = \max\{\| M d^{v+1} \\ - F^{\text{int}}(d_1^{v+1}, \ldots, d_i^{v+1}, \ldots, d_N^{v+1}) - F^{\text{ext}} \|_2\} \leq \epsilon \tag{7}$$

or

$$\max\{\| d^{v+1}(t) - d^v(t) \|\} \leq \epsilon \tag{8}$$

for some small positive constant ϵ.

For the convergence analysis of the WR method, see [24]. In the proposed multilevel method, the WR serves as a smoother to capture the high-frequency motions of the system.

2.2 POD-Based Variational Space-Time Multiscale Method

The multilevel method consists of a fine-scale smoothing scheme aimed at capturing the high-frequency motions of the system and a coarse-scale solution to resolve smooth features.

One of the main challenges in developing an efficient multilevel approach is to construct the coarse-scale problem. In the present paper, the coarse-grained equations are constructed directly from the fine scale using Hamilton's principle on the subspace of the coarse-scale functions. Let e be the coarse-scale correction. The updated fine-scale solution at a certain time step is given by $d^{v+1} = d^v + Qe$, where d is at fine scale. The Lagrangian of the system is expressed as

$$L(Qe, Q\dot{e}) = \tfrac{1}{2}(\dot{d}^v + Q\dot{e})^T M(\dot{d}^v + Q\dot{e}) - V(d^v + Qe) \quad (9)$$

where Q is the coarse-to-fine prolongation operator.

Applying Lagrange's equations, the resulted coarse-grid problem is

$$\begin{cases} Q^T M Q\ddot{e} - Q^T F^{\text{int}}(d^v + Qe) \\ \qquad = -Q^T M\ddot{d}^v + Q^T F^{\text{ext}} \\ e(0) = 0 \\ \dot{e}(0) = 0 \end{cases} \quad (10)$$

Equation (10) can be integrated explicitly or implicitly. For the algorithmic details of the nonlinear space-time multilevel method, see [11].

In the present paper, POD modes are used to construct the prolongation operator, Q. Briefly speaking, POD seeks a subspace to minimize the total square distance between the original points and their projecting points. POD modes are optimal in a least-squares sense with respect to the energy content of the dynamic behavior of the system.

From a numerical simulation using Eq. (1), the time histories of the coordinates that determine the positions of all atoms are saved. Then, the data are collected in an observation matrix Φ as

$$\Phi_{NN\times J} = \begin{bmatrix} d^1(1) & \ldots & d^1(j) & \ldots & d^1(J) \\ \vdots & \vdots & \vdots & \vdots & \vdots \\ d^i(1) & \ldots & d^i(j) & \ldots & d^i(J) \\ \vdots & \vdots & \vdots & \vdots & \vdots \\ d^{NN}(1) & \ldots & d^{NN}(j) & \ldots & d^{NN}(J) \end{bmatrix} \quad (11)$$

$$i = 1, 2, ..., NN; \quad j = 1, 2..., J$$

where $d^i(j)$ is the jth snapshot of the ith degree of freedom motion, J is the number of the snapshots, and NN is the number of total degrees of freedom of the molecular model.

There is a choice between computing the singular value decomposition of Φ or Φ^T for finding POD modes, which depends on the relative size of NN and J. In the field of principal component analysis, the first method is called the R-method and second is the Q-method [25]. The modal vectors produced by the two methods can be shown to differ by only a constant scaling matrix. In this work, the R-method is selected since the number of degrees of the system is not very high. The R-method is described below.

The singular value decomposition of Φ is given as

$$\Phi = U\Sigma V^T \quad (12)$$

where U is a unitary matrix of dimension $NN \times n$ and V is also a unitary matrix of dimension $J \times n$. One may select n, and typically, n will be much less than J. Note that

$$U^T U = I_{n\times n}, \qquad V^T V = I_{n\times n} \quad (13)$$

and Σ is a diagonal matrix of singular values, i.e.,

$$\Sigma_{n\times n} = \begin{bmatrix} \sigma_1 & & & & \\ & \sigma_2 & & & \\ & & \cdot & & \\ & & & \cdot & \\ & & & & \sigma_n \end{bmatrix} \quad (14)$$

where

$$\sigma_1 \geq \sigma_2 \geq ....\sigma_n \quad (15)$$

and the correlation matrix ρ is constructed as

$$\rho \equiv \Phi\Phi^T = U\Sigma^T V^T V\Sigma U^T \quad (16)$$

Substituting Eq. (13) into the above equation, we have

$$\rho = U\Sigma^T\Sigma U^T \quad (17)$$

and U is the eigenvector of the matrix ρ.

It is well known that the success of the POD methodology depends on the choice of the excitation used to obtain the snapshots. A certain amount of numerical experimentation may be required to determine an effective excitation to calculate the snapshots.

The prolongation operator, Q, is then selected as

$$Q = U \quad (18)$$

3. NUMERICAL RESULTS

In this section, a performance study is conducted on a model problem of a chain of ten monomers of α-D-glucopyranose ($C_6H_{12}O_6$). Each monomer has 24 atoms with 6 carbon atoms, 6 oxygen atoms, and 12 hydrogen atoms. For the ten-monomer system, there are $24 \times 10 - 3 \times 9 = 213$ atoms. Two of these atoms are fixed and one is attached to the tip of the atomic force microscope (AFM) and only allowed to move in one direction as shown in Fig. 1. The system, totally, has 631 degrees of freedom. The stiffness of the AFM cantilever is chosen to be $k_s = 10pN/\text{Å}$. In the simulations, the AFM base motion is prescribed along the z direction as

$$B(t) = A\sin(2\pi f t)$$

where A and f are the excitation amplitude and frequency, respectively. In the simulation, we choose $A = 1$ Å and $f = 100$ GHz.

The interactions between atoms are described by the following potential energy function:

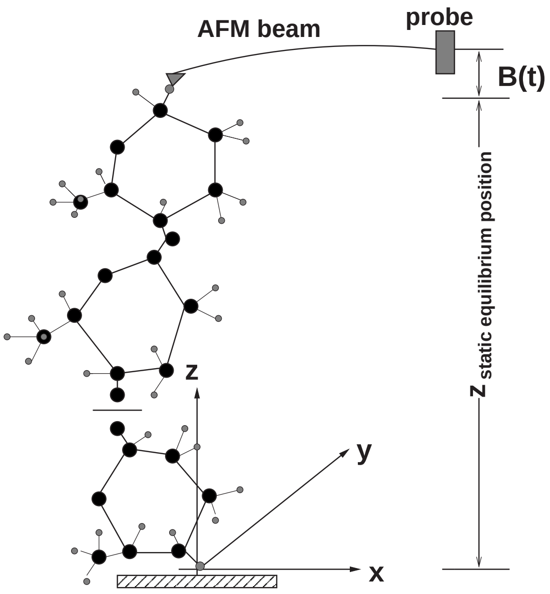

FIGURE 1. Schematic diagram for stretching of the molecule by an AFM

$$\begin{aligned} U = & \sum k_b(b-b_0)^2 + \sum k_\theta(\theta-\theta_0)^2 \\ & + \sum_{\text{torsions}} \sum_{n} k_\phi[1+\cos(n\phi-\delta)] \\ & + \sum_{i\neq j}\left(\frac{A_{ij}}{r_{ij}^{12}} - \frac{B_{ij}}{r_{ij}^{6}}\right) + \sum_{i\neq j} K_{\text{coul}}\frac{e_i e_j}{\epsilon r_{ij}} \end{aligned} \qquad (19)$$

where each term corresponds to different kinds of interactions, bond stretching, bend angle, torsion angle, Van der Waals, and electrostatic interaction, respectively. All of the potential terms are functions of the internal coordinates: bond length, b, bond angle, θ, and dihedral angle, ϕ; r_{ij} is the distance between atom i and atom j. The force-field parameters (k_b, k_θ, k_ϕ, A_{ij}, B_{ij}, ϵ, e_i, and e_j), equilibrium bond length (b_0), and equilibrium bend angle (θ_0) are obtained from [26].

The temperature is related to the average kinetic energy of the system by

$$\text{Temp} = \frac{2}{3Nk_b}\langle E_k\rangle \qquad (20)$$

where N is the number of atoms, k_b is Boltzmann's constant, and $\langle E_k\rangle$ is the time-averaged kinetic energy.

Figure 2 and 3 show the temperature and z coordinate of the AFM tip obtained by the POD-based reduced-order model compared to the original explicit Newmark results, respectively. The allowable maximum time step for the original explicit Newmark results is 0.001 ps.

To calculate POD modes, the snapshots are generated by first exciting the system by a sine sweep with lower- and upper-limit frequencies of ω_{low} and ω_{up}, given as

$$B(t) = A_{\text{sweep}}\sin(\omega_{\text{low}} + \frac{(\omega_{\text{up}} - \omega_{\text{low}})t}{2T})t$$

where T is the sweep period. In this example, the sine-sweep frequency range is chosen as 0–$2T$ Hz, $A_{\text{sweep}} = 1$ Å, and the time duration is $T = 100$ ps.

Figures 2 and 3 indicate that 50 modes are necessary for POD-based reduced-order model to provide a good approximation to the original explicit results. With 50 modes in the POD-based reduced-order model, the time-integration time step can be 10 times larger compared to the original explicit

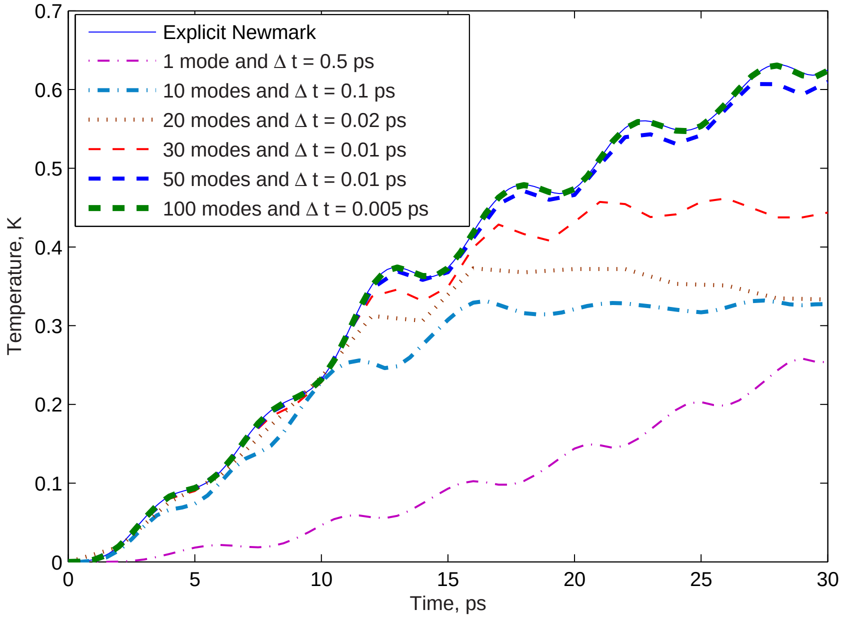

FIGURE 2. Temperature results obtained by POD-based ROM with different numbers of modes included

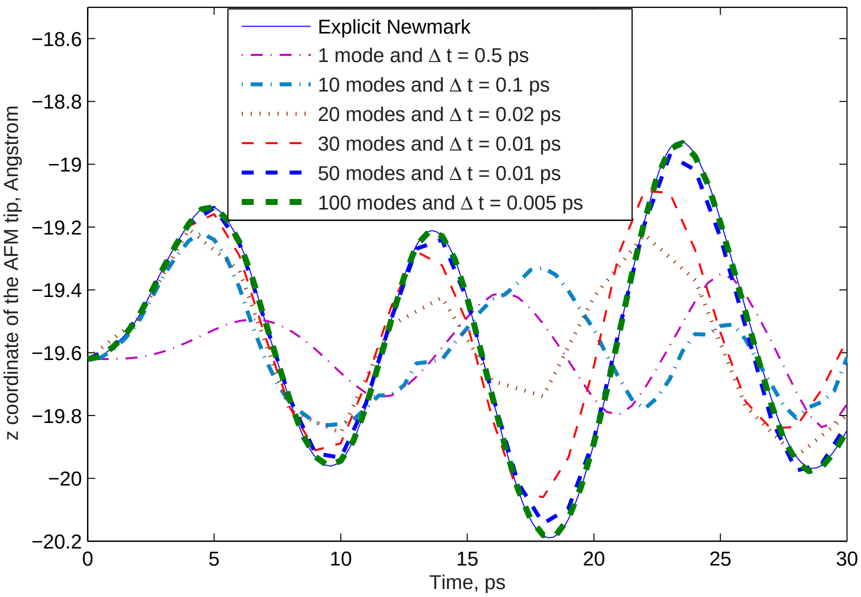

FIGURE 3. Time history of z coordinate of the AFM tip obtained by POD-based reduced-order model

Newmark results while retaining the desired accuracy. Thus, the computational cost can be reduced by a factor of 10.

Figures 4 and 5 show the time histories of the temperature and z coordinate of the AFM tip obtained by the waveform relaxation method described in Eq. (6) compared to the original explicit Newmark results. Each window has only one time step. The iteration is terminated when $\max\{\| d^{v+1}(t) - d^{v}(t) \|\} \leq 10^{-3}$ for all times. With waveform relaxation, the maximum time step is up to 0.2 ps for the desired accuracy, and the iteration number for convergence is about 651. Comparing the CPU time used, it is found that the simulation can be reduced by a factor of 35.

Figures 6–8 show the temperature and z coordinate of the AFM tip obtained by POD-based space-time multilevel method with 30 modes, 10 modes, and 1 mode, respectively. Note that the results are almost the same as the original explicit results with 10 or 30 modes included. The results with 1 mode are reasonably good. However, recall that for the POD-based reduced-order model, up to 50 modes are needed for the desired accuracy of the results. Because of the waveform-relaxation smoothing procedure at fine scale, even fewer POD modes in the coarse-grained model still provide a good approximation to the original results. With fewer POD modes, the integration time step can be further increased. With one mode included, the time step can be 0.5 ps. Compared to the POD-based reduced-order model, the POD-based space-time multiscale method is much more efficient.

Figure 9 illustrates the relative CPU time on a single-processor machine by the POD-based space-time multilevel method compared to the time cost of time marching the original system by the explicit Newmark method. As the number of modes included decreases, the allowable integration time step increases. With the POD-based space-time multilevel method, the simulation can be orders of magnitude faster than the original explicit time-marching method.

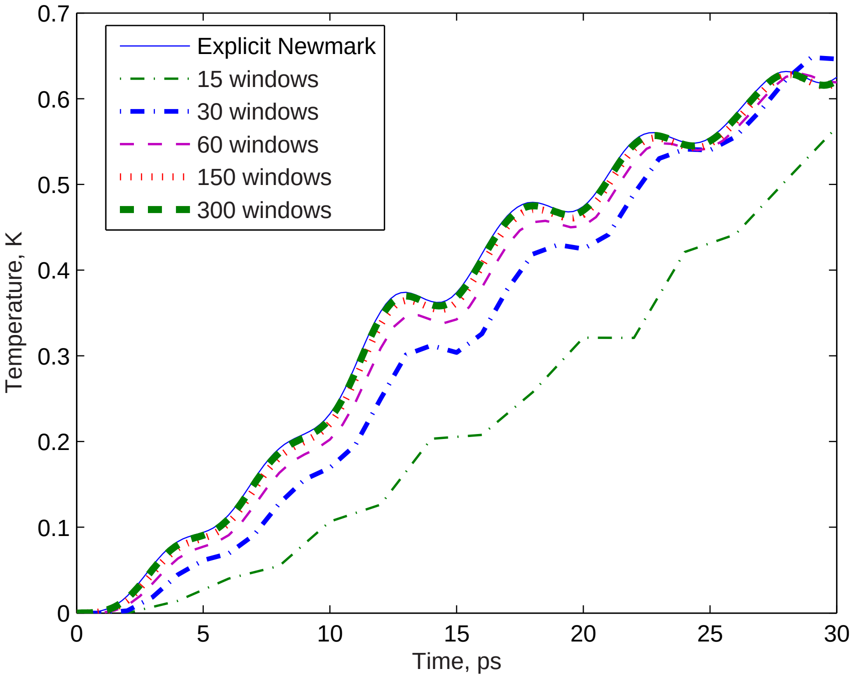

FIGURE 4. Temperature results obtained by waveform-relaxation method. Each window only includes one time step

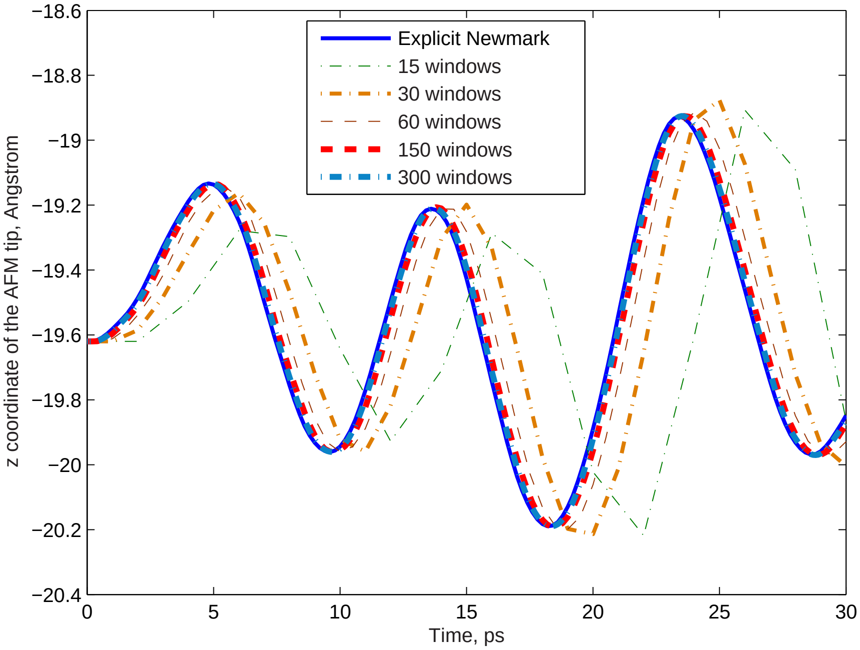

FIGURE 5. Time history of z coordinate of the AFM tip obtained by waveform-relaxation method. Each window only includes one time step

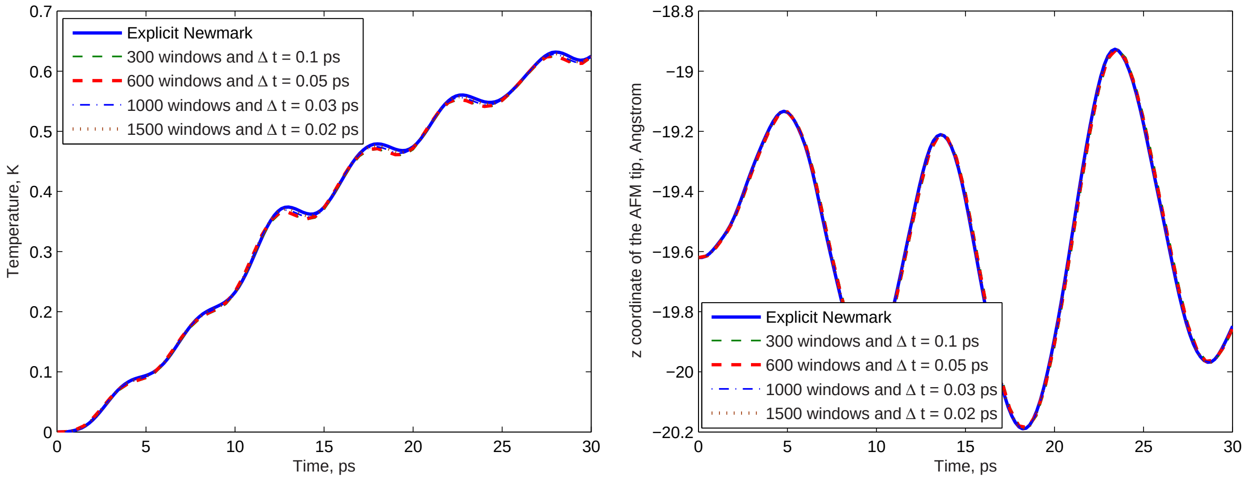

(a) Temperature

(b) z coordinate of the AFM tip

FIGURE 6. Results obtained by POD-based space-time multilevel method with 30 modes included

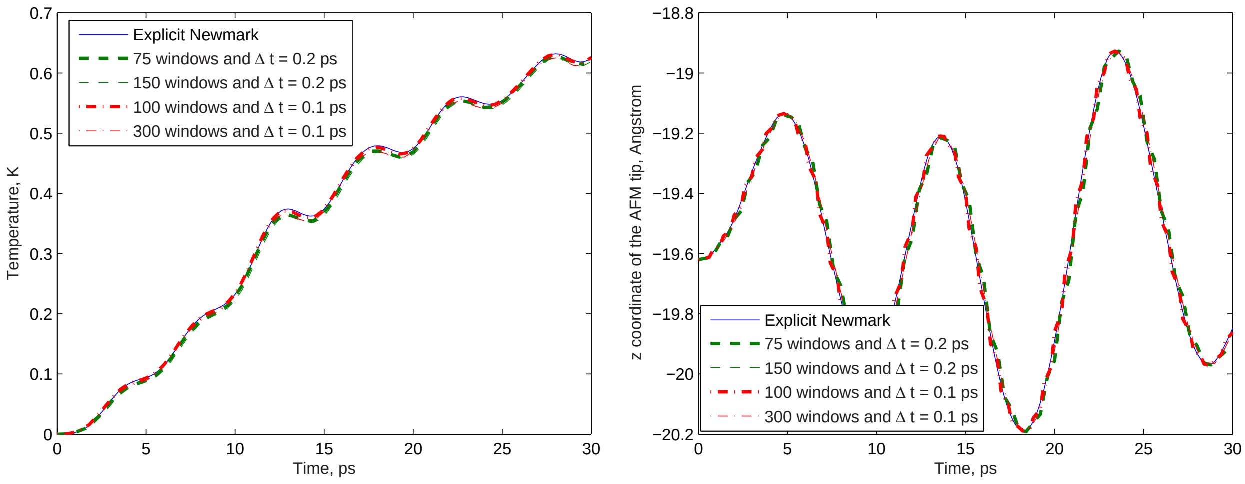

(a) Temperature (b) z coordinate of the AFM tip

FIGURE 7. Results obtained by POD-based space-time multilevel method with ten modes included

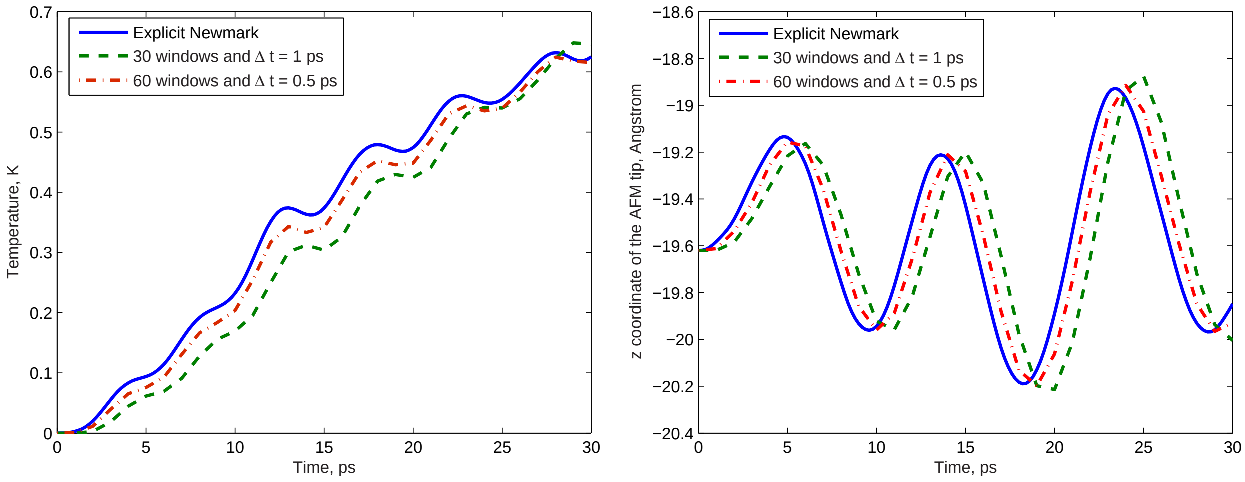

(a) Temperature (b) z coordinate of the AFM tip

FIGURE 8. Results obtained by POD-based space-time multilevel method with one mode included

4. CONCLUSIONS

A novel multiscale method that combines the waveform-relaxation and POD-based reduced-order models within a framework of the space-time multilevel method has been developed. In this framework, the waveform-relaxation smoothing captures the oscillatory response of the high-frequency motions and a POD-based reduced, order model resolves the smooth features of the system. The formulation of the coarse-grained model is based on the variational approach derived from the Hamilton's principle. The time integration is performed in windows using the Newmark predictor-corrector method. The numerical example of modeling a chain of glucopyranose

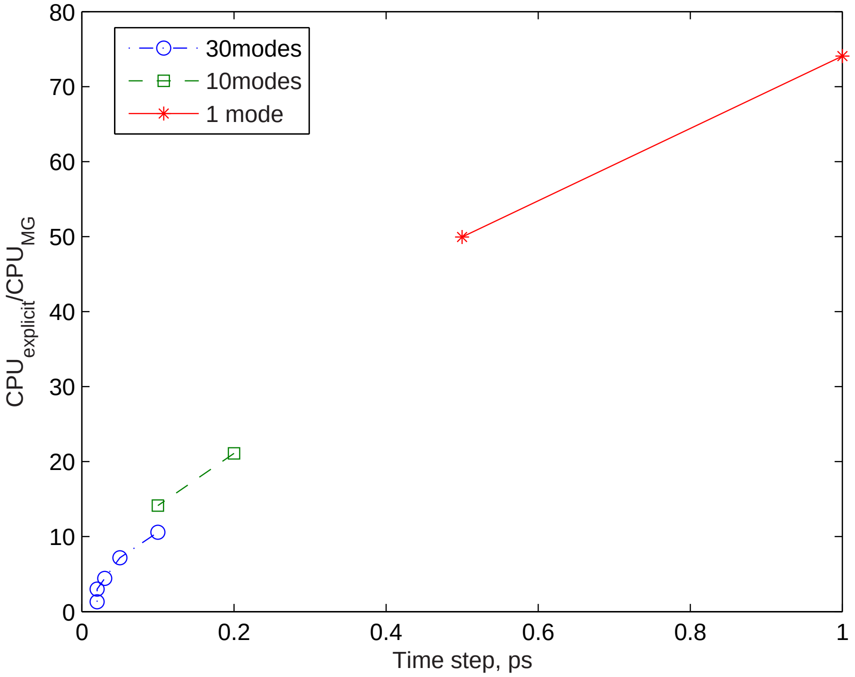

FIGURE 9. Relative time versus time step for different numbers of modes included in POD-based space-time multi-level method

monomers shows significant time savings compared to standard explicit integrators and the POD-based reduced-order model. Possible parallel implementation of the proposed method will further speed up the simulation. Future work will be done on the convergence analysis of the method.

REFERENCES

1. Mccammon, J. A., and Harvey, S. C., *Dynamics of Proteins and Nucleic Acids*, Cambridge University Press, Campbridge, England, 1987.
2. Kitao, A., and Go, N., Conformational dynamics of polypeptides and proteins in the dihedral angle space and in the cartesian coordinate space: normal mode analysis of deca-alanine, *J. Comput. Chem.* **12**(3):359–368, 1991.
3. Ewald, P. P., Die berechnung optischer und elektrostatischer gitterpotentilae, *Annu. Phys.* **64**:253–287, 1921.
4. Eastwood, J. W., and Hockney, R. W., Shaping the force law in two-dimensional particle mesh models, *J. Comput Phys.* **16**:342–359, 1974.
5. Greengard, L., and Rokhlin, V., A fast algorithm for particle simulations, *J. Comput. Phys.* **73**:325–348, 1987.
6. Brooks, B. R., Bruccoleri, R. E., Olafson, B. D., States, D. J., Swaminathan, S., and Karplus, M., CHARMM: A program for macromolecular energy, minimization and dynamic simulation, *J. Comput. Chem.* **4**(2):187–217, 1983.
7. Frenkel, D., and Smit, B., *Understanding Molecular Simulations: From Algorithms to Applications, 2nd ed.* Academic Press, New York, 2002.
8. Andersen, H. C., Rattle: a velocity version of the shake algorithm for molecular dynamics calculations, *J. Comput. Phys.* **52**:24–34, 1983.
9. Tuckerman, M., and Berne, B. J., Reversible multiple time scale molecular dynamics, *J. Chem. Phys.* **97**(3):1990–2001, 1992.
10. Barash, D., Yang, L., Qian, X., and Schlick, T., Inherent speedup limitations in multiple time step/particle mesh Ewald algorithms, *J. Comput. Chem.* **24**:77–88, 2002.
11. Waisman, H., and Fish, J., A space-time mul-

tilevel method for molecular dynamics simulations, *Comput. Methods Appl. Mech. Eng.* **195**:6542–6559, 2006.

12. Burrage, K., *Parallel and Sequential Methods for Ordinary Differential Equations*. Oxford University Press, London, 1995.
13. Saguia, C., and Darden, T., Multigrid methods for classical molecular dynamics simulations of biomolecules, *J. Chem. Phys.* **114**(15):6578–6591, 2001.
14. Robert D. Skeel and Ismail Tezcan and David J. Hardy, Multiple Grid Methods for Classical Molecular Dynamics, *J. Comput. Chem.* **23**(6):673–684, 2002.
15. Sutmann, G., and Steffen, B., A particle-particle particle-multigrid method for long-range interactions in molecular simulations, *Comp. Phys. Commun.* **169**:343–346, 2005.
16. Rudd, R. E., and Broughton, J. Q., Coarse-grained molecular dynamics and the atomic limit of finite elements, *Phys. Rev. B*. **58**(10):R5893–R5896, 1998.
17. Feeny, B. F., and Kappagantu, R., On the physical interpretation of proper orthogonal modes in vibrations, *J. Sound & Vib.* **211**(4):607–616, 1998.
18. Racindra, B., Comments on ”On the physical interpretation of proper orthogonal modes in vibrations”, *J. Sound & Vib.* **219**(1):189–192, 1999.
19. Kerschen, G., and Golinval, J. C., Physical interpretation of the proper orthogonal modes using singular value decomposition, *J. Sound & Vib.* **249**(5):849–865, 2002.
20. Li, A., and Dowell, E. H., Modal reduction of mathematical models of biological molecules, *J. Comput. Phys.* **211**:262–288, 2006.
21. Saleh, R. A., and White, J. K., Accelerating relaxation algorithms for circuit simulation using waveform-newton and step-size refinement, *IEEE Trans. Comput.-Aided Des. Integr. Circuits Syst.* **9**(9):951–958, 1990.
22. Lumsdaine, A., and Reichelt, M. W., Waveform iterative techniques for device transient simulation on parallel machines, *6th SIAM Conference on Parallel Processing for Scientific Computing, Norfolk, VA*, 1993.
23. Hughes, T. J. R., *The Finite Element Method: Linear Static and Dynamic Finite Element Analysis*. Dover, New York, 1987.
24. Miekkala, U., and Nevanlinna, O., Convergence of dynamic iteration methods for initial value problems. *SIAM J. Sci. Stat. Comput.* **8**(4):459–482, 1987.
25. Jackson, J. E., *A User's Guide to Principal Components*. Wiley, New York, 1991.
26. Kuttel, M., Brady, J. W., and Brady, K. J., Carbohydrate solution simulations: Producing a force field with experimentally consistent primary alcohol rotational frequencies and populations. *J. Comput. Chem.* **23**(13):1236–1243, 2001.